# A Study on the Control Model Identification and $H_\infty$ Controller Design for Tandem Cold Mills

**Man Hyung Lee***
*School of Mechanical Engineering and ERC/Net Shape & Die Manufacturing, Pusan National University, Pusan 609-735, Korea*
**Yu Shin Chang, In-Soo Kim**
*Graduate School of Mechanical and Intelligent Systems Engineering, Pusan National University, Pusan 609-735, Korea*

This paper considers the control model identification and $H_\infty$ controller design for a tandem cold mill (TCM). In order to improve the performance of the existing automatic gauge control (AGC) system based on the Taylor linearized model of the TCM, a new mathematical model that can complement the Taylor linearized model is constructed by using the N4SID algorithm based on subspace method and the least squares algorithm based on ARX model. It is shown that the identified model has dynamic characteristics of the TCM than the existing Taylor linearized model. The $H_\infty$ controller is designed to have robust stability to the system parameters variation, disturbance attenuation and robust tracking capability to the set-up value of strip thickness. The $H_\infty$ servo problem is formulated and it is solved by using LMI (linear matrix inequality) techniques. Simulation results demonstrate the usefulness and applicability of the proposed $H_\infty$ controller.

**Key Words** : Tandem Cold Mill, N4SID (Numerical algorithms for Subspace State Space System IDentification), LMI-based $H_\infty$ Control, Taylor Linearized Model, Interstand Interference

## 1. Introduction

In tandem cold rolling, the quality demands of cold rolled strip, including small tolerances on the cold rolled gauge, flatness, stress distribution of strip and strip roughness, have been increasing with the development of industrial technology related to the steel industry. Strip quality in tandem cold rolling depends on the performance of the automatic gauge control (AGC) system, so there has been a lot of research related to the development of AGC system to improve the performance of the existing system. Various control methods such as BISRA AGC, feedforward AGC have been applied for the control of strip thickness and tension in tandem cold rolling. Recently, AGC systems designed by using modern control theories such as noninteractive control, LQ and LQG control, robust control have been investigated, based on the Taylor linearized model (Hoshino, et al., 1997; Lee, et al., 1998; Shin, et al., 1998; Geddes, et al., 1998). In the design of robust control system for the tandem cold mill (TCM), it is very important to construct an independent linear control model of each stand. This model also must have interstand interference property (that is some parameters of the TCM such as strip thickness, roll gap and roll speed are affected greatly by the tension of each stand) of the TCM. The Taylor linearized model just depicts all stands of the TCM as a multivaria-

* Corresponding Author,
**E-mail** : mahlee@hyowon.pusan.ac.kr
**TEL** : +82-51-510-2331 ; **FAX** : +82-51-512-9835
School of Mechanfical Engineering and ERC/Net Shape & Die Manufacturing, Pusan National University. San 30, Jangjeon-dong, Keumjung-ku, Pusan 609-735, Korea. (Manuscript **Received** July 6, 2000; **Revised** May 10, 2001)

ble system (Lee, et al., 1999), so there is a limit to design an independent robust controller for each stand based on this linear model.

The objective of this paper is to construct the independent linear model of the five-stand TCM using model identification method and to design the $H_\infty$ controller to improve the strip quality. The linear models of all the stands of TCM are identified by the N4SID (numerical algorithms for subspace state space system identification) algorithm (Van Overschee, et al., 1994; Verhaegen, et al., 1992) based on subspace method and the least squares algorithm (Ljung, 1999) based on a ARX model, and these are compared to the existing Taylor linearized model to evaluate the accuracy of the identified models. It is very important to construct the explicit mathematical model of the TCM to design the $H_\infty$ controller that has robust stability, disturbance attenuation and robust tracking properties. The nominal models are identified from input and output data without uncertainties and then the uncertain models are identified from input and output data containing uncertainties. For designing the $H_\infty$ controller that satisfies the given performances, the $H_\infty$ servo problem (Hozumi, et al., 1997) is applied to the identified model. The $H_\infty$ servo problem is modified as a usual $H_\infty$ control problem with an internal model that contains the mode of reference input model, and the LMI-based solution for the $H_\infty$ control is applied to solve the modified $H_\infty$ problem (Gahinet, et al., 1994; Gahinet, 1996). The $H_\infty$ controller designed with the identified TCM model is assessed by computer simulations and the results demonstrate the usefulness and the feasibility of the proposed approach to the tandem cold rolling process.

The organization of this paper is as follows. The next section presents the identified models of the TCM by using the N4SID and the least squares methods. The $H_\infty$ controller based on LMI technique with these identified model is designed and simulation results are discussed in section 3, finally, the conclusion is presented in section 4.

## 2. Model Identification

The TCM shown in Fig. 1 is consisted of five stands, in which strip is rolled continuously from the first stand to the last one. A distinctive feature of the TCM is that there are interstand interference in all stands, i.e., every rolling phenomenon occurred in one stand affects another by the interstand tension. Therefore, it is necessary to consider interstand interference in the tandem cold rolling process to construct an accurate linear model. For the thickness control in the tandem cold rolling, the AGC system which is designed based on the Taylor linearized model of the TCM is set up in each stand. Because the Taylor linearized model is represented by the first order differential equation, and just depicts the TCM as one multivariable system, it is very difficult to adjust the controller gain of each stand to design independent robust thickness control system based on this Taylor linearized model, especially under the uncertainties of rolling process.

In this study, model identification methods are applied to the five-stand TCM in order to construct an independent linear model for each stand. The input and output data for identifying linear models of the TCM are generated from the nonlinear TCM simulator that was developed by MATLAB software, acting as a realistic environment of the tandem cold rolling process (Lee, et al., 1998). These data also must have natural dynamic characteristics of tandem cold rolling process, such as interstand interference and interstand time-delay. Especially in the case of a multivariable system, the selection of the input and output variables in model identification is very important to determine the model structure. Therefore, we must understand the interrelation between input (roll gap, roll speed) and output

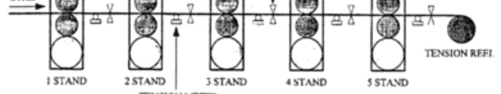


Fig. 1 A five-stand tandem cold mill

(delivery-strip thickness, backward tension) of each stand, and determine the suitable input and output variables for identifying linear model from these relations. The input and output variables for identifying linear model of the each stand are shown in Table 1. Input variables $S_i$ and $V_{Ri}$ are the roll gap and roll speed of stand $i$. Maximum length sequence (Ljung, 1999) which approximates white noise is used as the input signal for model identification. As shown in Fig. 2 maximum length sequence is the pseudo-random binary (two-level) signal with an arbitrary period. The input variables, i.e. roll gap and roll speed generated in the form of maximum length

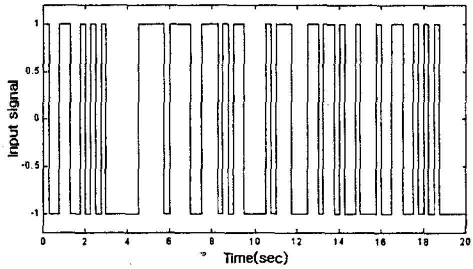


**Fig. 2** Input signal (maximum length sequence) for model identification

**Table 1** The input and output variables for model identification of the TCM

| Stand No. | Input variables | Output variables |
|---|---|---|
| 1 | $S_1$, $V_{R1}$, $S_2$, $V_{R2}$ | $h_1$ |
| 2 | $S_1$, $V_{R1}$, $S_2$, $V_{R2}$, $S_3$, $V_{R3}$ | $h_2$, $\tau_{b2}$ |
| 3 | $S_2$, $V_{R2}$, $S_3$, $V_{R3}$, $S_4$, $V_{R4}$ | $h_3$, $\tau_{b3}$ |
| 4 | $S_3$, $V_{R3}$, $S_4$, $V_{R4}$, $S_5$, $V_{R5}$ | $h_4$, $\tau_{b4}$ |
| 5 | $S_4$, $V_{R4}$, $S_5$, $V_{R5}$ | $h_5$, $\tau_{b5}$ |

sequence were used for model identification of the TCM. Initial set-up values of the TCM are shown in Table 2 and output data are generated from the nonlinear TCM simulator with maximum length sequence type input signal.

### 2.1 Identified nominal model of the TCM

We applied the N4SID method based on subspace model identification and the least squares method based on ARX model to identify a linear control model of the TCM, and determined the better method from the results. The identified model form is a multivariable LTI (linear time invariant) state space model. In model identification, firstly, the nominal model of each stand is identified from the input and output data without uncertainties, and secondly, the model is identified from the input and output data that contained uncertainties, such as the variation of entry-strip thickness and roll eccentricity, occurred in the tandem cold rolling.

In this section, the nominal model of the TCM is identified by using the N4SID and the least squares methods with the input and output data that does not contain the uncertainties. The data is generated in the nonlinear TCM simulator, and the data sampling time is 0.04 seconds and the total period for generating the input and output data is 20 seconds. Interstand interference and interstand time-delay in the tandem cold rolling are also considered when the data are generated. The identified model from the N4SID method is in the form of discrete-time LTI state space model as follows.

$$\begin{aligned} x(k+1) &= Ax(k) + Bu(k) \\ y(k) &= Cx(k) + Du(k) \end{aligned} \tag{1}$$

**Table 2** Initial set-up values of the TCM

| Parameters | Unit | Stand 1 | Stand 2 | Stand 3 | Stand 4 | Stand 5 |
|---|---|---|---|---|---|---|
| Entry-strip thickness ($H_i$) | mm | 2.60 | 2.12 | 1.57 | 1.17 | 0.89 |
| Delivery-strip thickness ($h_i$) | mm | 2.12 | 1.57 | 1.17 | 0.89 | 0.80 |
| Forward tension ($\tau_{bi}$) | kgf/mm$^2$ | 0 | 12.7 | 17.1 | 23.0 | 24.1 |
| Backward tension ($\tau_{fi}$) | kgf/mm$^2$ | 12.7 | 17.1 | 23.0 | 24.1 | 6.7 |
| Work-roll radius ($R$) | mm | 273 | 273 | 292 | 292 | 292 |

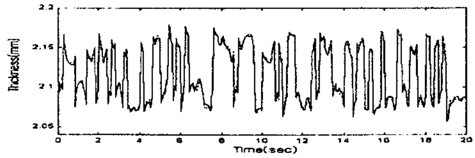

(a) Stand 1 delivery-strip thickness

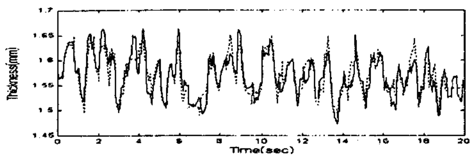

(b) Stand 2 delivery-strip thickness

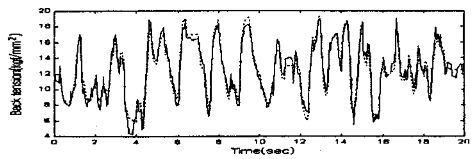

(c) Stand 2 backward tension

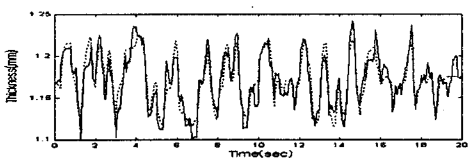

(d) Stand 3 delivery-strip thickness

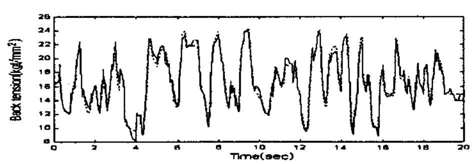

(e) Stand 3 backward tension

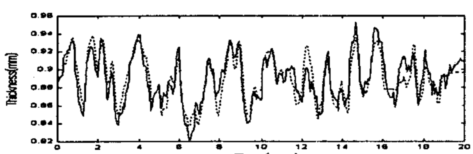

(f) Stand 4 delivery-strip thickness

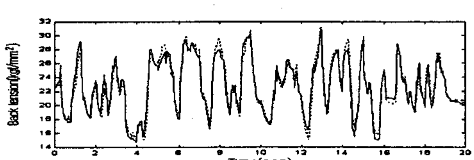

(g) Stand 4 backward tension

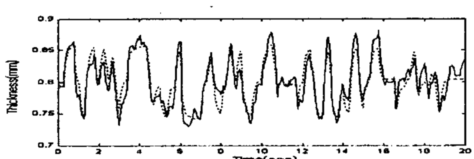

(h) Stand 5 delivery-strip thickness

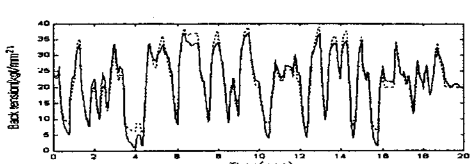

(i) Stand 5 backward tension

**Fig. 3** The identification results by using the N4SID method

As a result of the model identification by the N4SID method, all stands were identified as a MIMO (multi-input multi-output) system. In Fig. 3, the output signals of the identified model were compared to the output signals used in model identification with the N4SID method; a solid line is the output signal used in model identification and a dotted line is the output signal of the identified model by the N4SID method. The identification error of delivery-strip thickness in stand 1 is within $\pm 10$ $\mu$m, which is the least among the identification results of all stands. The identification errors of stand 2 and stands 3~5 are within $\pm 20$ $\mu$m and $\pm 40$ $\mu$m, respectively. In the identification error of backward tension, stands 2 and 3 are $\pm 2$kgf/mm$^2$, stand 5 is $\pm 6$kgf/mm$^2$, and stand 4 is $\pm 3$kgf/mm$^2$, respectively.

The linear model identified by using the least squares method is in the form of ARX model, discrete-time transfer function, as follows.

$$A(z^{-1})\,y(t) = B(z^{-1})\,u(t) + e(t) \qquad (2)$$

where $A(z^{-1}) = 1 + a_1 z^{-1} + a_2 z^{-2} + \cdots + a_n z^{-n}$, $B(z^{-1}) = b_1 z^{-1} + b_2 z^{-2} + \cdots + b_m z^{-m}$, $u(t)$, $y(t)$

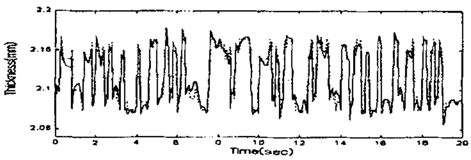


(a) Stand 1 delivery-strip thickness

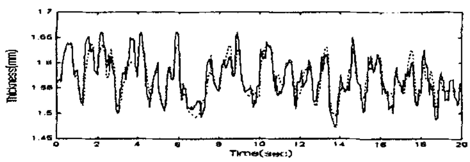


(b) Stand 2 delivery-strip thickness

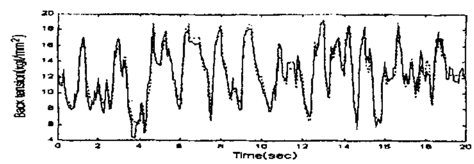


(c) Stand 2 backward tension

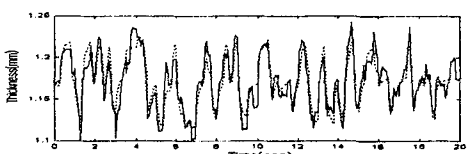


(d) Stand 3 delivery-strip thickness

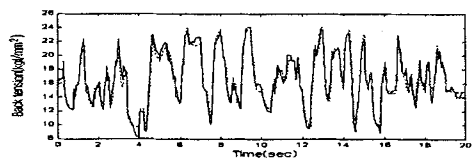


(e) Stand 3 backward tension

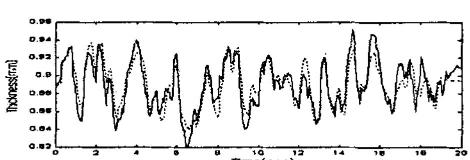


(f) Stand 4 delivery-strip thickness

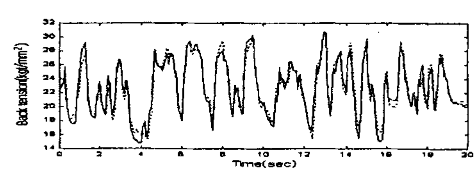


(g) Stand 4 backward tension

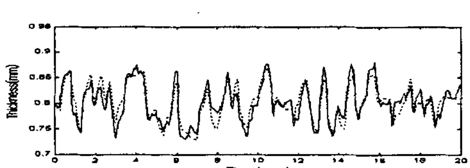


(h) Stand 5 delivery-strip thickness

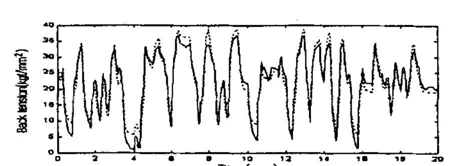


(i) Stand 5 backward tension

**Fig. 4** The identification results by using the least squares method

and $e(t)$ are input, output, and white noise, respectively.

As a result of the identification using the least squares method, stand 1 was identified as a MISO (multi-input single-output) system, and the other stands were identified as MIMO systems. In Fig. 4, a solid line represents the output signal used in model identification and a dotted line does the output signal of the identified model by the least squares method. The identification error of stand 1 is within $\pm 20$ $\mu$m and those of the others are approximately within $\pm 40$ $\mu$m. From the identification results by the N4SID and the least squares methods, we concluded that the identification results of the N4SID method were more accurate than those of the least squares method, and the identified model of the N4SID method had model structure of lower order than that of the least squares method. The identified TCM models of the N4SID method that were realized in the form of discrete-time linear state space model are shown in Table 3.

**Table 3** The identified linear models of the TCM by the N4SID method

| Identified model | | Discrete-time state space model | Eigenvalues |
|---|---|---|---|
| Stand 1 | A | $\begin{bmatrix} 0.8112 & -0.3552 \\ 0.5261 & -0.2076 \end{bmatrix}$ | 0.5727, 0.0319 |
| | B | $\begin{bmatrix} -0.1686 & 3.6\times10^{-5} & -0.0133 & 1.7\times10^{-4} \\ -6.6196 & 1.4\times10^{-5} & -0.0302 & 4.4\times10^{-3} \end{bmatrix}$ | |
| | C | $\begin{bmatrix} 0.4014 & 0.9166 \end{bmatrix}$ | |
| | D | $\begin{bmatrix} -0.0103 & 6.6\times10^{-6} & -0.0397 & 5.8\times10^{-6} \end{bmatrix}$ | |
| Stand 2 | A | $\begin{bmatrix} 0.0353 & -0.2135 & -0.5712 \\ -0.7343 & 0.4421 & 0.3535 \\ 0.6050 & 0.1930 & 0.6986 \end{bmatrix}$ | 0.2541+j0.2565, 0.2541−j0.2565, 0.6679 |
| | B | $\begin{bmatrix} -17.0905 & 0.0028 & 3.5882 & 0.0099 & -0.7175 & 0.0005 \\ -24.3410 & -0.0099 & 14.2934 & 0.0248 & -1.1045 & -0.0001 \\ 22.3867 & 0.0002 & -7.2790 & -0.0170 & 1.0240 & -0.0001 \end{bmatrix}$ | |
| | C | $\begin{bmatrix} 0.0395 & 0.0056 & 0.0066 \\ 0.2678 & 0.8639 & -0.4184 \end{bmatrix}$ | |
| | D | $\begin{bmatrix} 0.3515 & 0.0001 & 0.0224 & -0.0002 & -0.0275 & 0.0 \\ -2.5667 & -0.0029 & 0.0433 & 0.0039 & 0.2328 & -0.0003 \end{bmatrix}$ | |
| Stand 3 | A | $\begin{bmatrix} 1.0003 & -0.3227 & 0.1298 \\ -0.0092 & 0.6168 & 0.8345 \\ 0.3942 & -0.3015 & -0.0615 \end{bmatrix}$ | 0.7013+j0.0926, 0.7013−j0.0926, 0.1530 |
| | B | $\begin{bmatrix} -31.2482 & 0.0049 & -6.4627 & 0.0083 & 0.1174 & -0.0005 \\ 23.0726 & 0.0051 & -75.7367 & -0.0162 & -0.2172 & 0.0148 \\ -94.7398 & 0.0003 & -5.7388 & 0.0417 & -1.8178 & 0.0051 \end{bmatrix}$ | |
| | C | $\begin{bmatrix} -0.0034 & 0.0104 & 0.0139 \\ -0.3561 & -0.7379 & 0.5713 \end{bmatrix}$ | |
| | D | $\begin{bmatrix} 0.7556 & 2.3\times10^{-5} & 0.3604 & -0.0003 & -0.0729 & -9.1\times10^{-5} \\ 4.8772 & -0.0024 & 1.6461 & -0.0003 & -1.9388 & -0.0006 \end{bmatrix}$ | |
| Stand 4 | A | $\begin{bmatrix} 0.8633 & -0.1038 \\ 0.7956 & 0.0554 \end{bmatrix}$ | 0.7432, 0.1755 |
| | B | $\begin{bmatrix} -4.7977 & 0.0029 & -4.2386 & -0.0026 & 1.1549 & -0.0001 \\ 41.3413 & 0.0033 & -21.0396 & -0.0152 & 1.9277 & 0.0024 \end{bmatrix}$ | |
| | C | $\begin{bmatrix} 0.0171 & -0.0074 \\ 0.0450 & -1.0112 \end{bmatrix}$ | |
| | D | $\begin{bmatrix} -0.0567 & 0.0 & 0.0194 & 0.0 & -0.0259 & 0.0 \\ 10.5333 & -0.0018 & 3.2995 & -0.0023 & -6.8935 & 0.0012 \end{bmatrix}$ | |
| Stand 5 | A | $\begin{bmatrix} 0.9149 & 0.6849 \\ -0.2113 & 0.0092 \end{bmatrix}$ | 0.7077, 0.2164 |
| | B | $\begin{bmatrix} -3.1280 & -0.0078 & 17.8801 & 0.0094 \\ -12.1699 & 0.0027 & -23.2223 & -0.0018 \end{bmatrix}$ | |
| | C | $\begin{bmatrix} -0.0040 & -0.0029 \\ 0.5186 & -0.8873 \end{bmatrix}$ | |
| | D | $\begin{bmatrix} -0.8704 & 7.0\times10^{-6} & 0.0184 & 0.0 \\ 24.2412 & -0.0028 & 0.8385 & -0.0010 \end{bmatrix}$ | |

### 2.2 Comparison of the identified model to the Taylor linearized model

The identified linear models are compared to the existing Taylor linearized model of the TCM. That is, the output data used for model identification, the output signal of the identified model and the output signal of the Taylor linearized model are compared with each other. The comparison results of the delivery-strip thickness of stands 1, 3 and 5 are shown in Fig. 5.

As shown in figures, delivery-strip thickness of the linear models that identified by using the N4SID method approached more closely to delivery-strip thickness of the TCM nonlinear model

**Table 4** The linearized error of the identified model and the Taylor linearized model

| Stand No. | Linearized error (difference of the linear model from nonlinear equations of the TCM) | | | | | |
|---|---|---|---|---|---|---|
| | Thickness error ($\mu$m) | | | Backward tension error (kgf/mm²) | | |
| | Identified model | | Taylor linearized model | Identified model | | Taylor linearized model |
| | Least squares | N4SID | | Least squares | N4SID | |
| 1 | −20∼20 | −10∼10 | −40∼40 | | | |
| 2 | −40∼50 | −50∼60 | −140∼130 | −2∼2 | −2∼2 | −12∼10 |
| 3 | −30∼40 | −30∼40 | −140∼100 | −2∼2 | −2∼2 | −13∼13 |
| 4 | −40∼40 | −30∼30 | −110∼100 | −2∼3 | −2∼3 | −14∼12 |
| 5 | −40∼40 | −40∼40 | −120∼140 | −6∼5 | −6∼5 | −30∼15 |

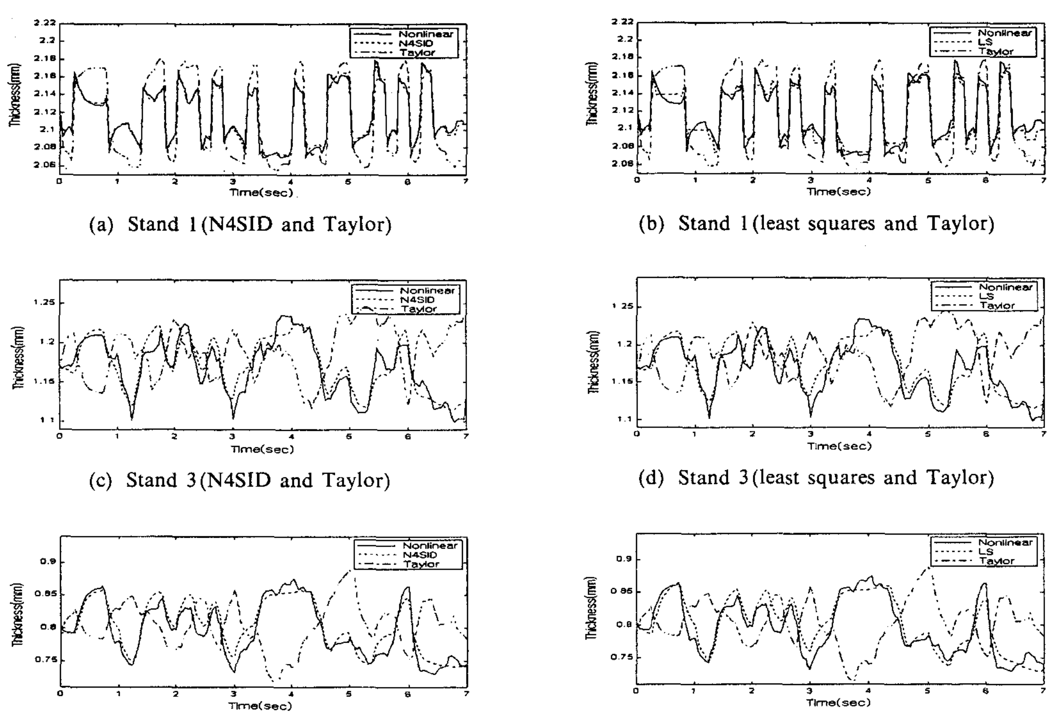


(a) Stand 1 (N4SID and Taylor)

(b) Stand 1 (least squares and Taylor)

(c) Stand 3 (N4SID and Taylor)

(d) Stand 3 (least squares and Taylor)

(e) Stand 5 (N4SID and Taylor)

(f) Stand 5 (least squares and Taylor)

**Fig. 5** Comparison results of the identified models and the Taylor linearized model than those of the identified models by the least squares method and the Taylor linearized model. The differences (that is the linearized errors of the identified models and the Taylor linearized model) between delivery-strip thickness of the Taylor linearized model and the identified models, and delivery-strip thickness of nonlinear simulation are within $\pm 50$ $\mu$m, $\pm 10$ $\mu$m and $\pm 20$ $\mu$m, respectively (see Table 4). From those comparison results, we concluded that the linear model identified by the N4SID method is the most accurate one with the distinctive dynamic characteristics of the tandem cold rolling process.

### 2.3 Identified model of the TCM with uncertainties

Disturbances in the tandem cold rolling, mainly roll eccentricity and the variation of entry-strip thickness, greatly affect the precision of strip thickness. Roll eccentricity occurs from the deformation of work-roll surface or discord between the geometrical center of roll and the axis of revolution. It affects the variation of strip thickness. In this section, we identified the linear models of all stands with the input and output data contaminated by these disturbances. Roll eccentricity was considered as a sinusoidal signal with the frequency dependent on the roll speed.

$$S_r = a\sin(2\pi a t) \qquad (3)$$

where $a$ ($=0.01$ mm) is a given value by considering delivery-strip thickness of each stand.

The uncertain variation of entry-strip thickness was generally considered as a composite sine with frequency of 0.1~2Hz and magnitude of 0.02 mm. The linear model of each stand was identified with the input and output data contained roll eccentricity and the variation of entry-strip thickness by using the N4SID and the least squares methods. The modeling errors that may happen in tandem cold rolling process were analyzed quantitatively by calculating errors between the identified models with uncertainties and the nominal models. The modeling error, caused by uncertainties, of stand 1 is described as an additive error function, which is given by (4), and its maximum singular value plot is shown in Fig. 6. It is necessary for the quantitative analysis of the modeling error at frequency domain to determine weighting functions in $H_\infty$ controller design.

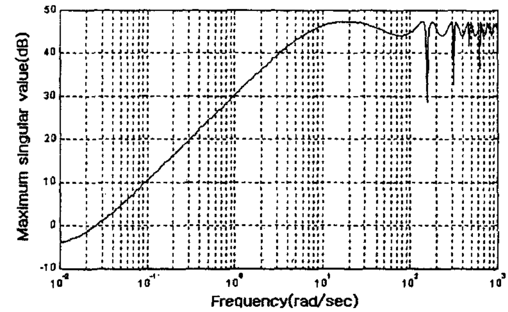


**Fig. 6** Maximum singular value plot of the modeling error function of stand 1

$$\left[\begin{array}{c|c} A & B \\ \hline C & D \end{array}\right] = \left[\begin{array}{cccc|cccc} 0.9199 & 0.7306 & 0.0 & 0.0 & 60.1259 & -0.0078 & 18.2803 & 0.0010 \\ -0.2065 & -0.0021 & 0.0 & 0.0 & -168.2814 & 0.0026 & -22.1756 & 0.0191 \\ 0.0 & 0.0 & 0.9149 & 0.6849 & -3.1280 & -0.0078 & 17.8801 & 0.0094 \\ 0.0 & 0.0 & -0.2113 & 0.0092 & -12.1699 & 0.0027 & -23.2223 & -0.0018 \\ \hline -0.0042 & -0.0037 & 0.0040 & 0.0029 & -1.3489 & 0.0 & -0.0021 & 0.0002 \\ 0.5166 & -0.9182 & -0.5186 & 0.8873 & 12.4583 & 0.0 & -0.0097 & -0.0017 \end{array}\right] \qquad (4)$$

## 3. $H_\infty$ Controller Design

The $H_\infty$ controller for strip thickness control under disturbances was designed based on the identified model of the TCM. In the tandem cold rolling process, the variation of entry-strip thickness and roll eccentricity were considered as disturbances and these greatly affect the strip thickness.

### 3.1 $H_\infty$ control

We applied the $H_\infty$ servo problem (Hozumi, et al., 1997) for designing the controller that

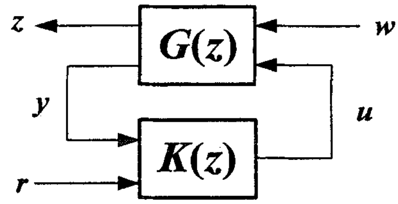


**Fig. 7** $H_\infty$ servo problem

achieves the robust tracking property (the delivery-strip thickness robustly tracks the reference input, i. e., the given set-up value without steady state error).

***$H_\infty$* servo problem** : Consider a two degrees-of-freedom control system depicted in Fig. 7.

$$G(z)=\left[\begin{array}{c|cc} A & B_1 & B_2 \\ \hline C_1 & D_{11} & D_{12} \\ C_2 & D_{21} & 0 \end{array}\right] \tag{5}$$

$$u=K(z)\begin{bmatrix} r \\ y \end{bmatrix} \tag{6}$$

For a given generalized plant $G(z)$ in (5) and a reference model, find a controller $K(z)$ in (6) satisfying the following specifications.

(1) $K(z)$ internally stabilizes $G(z)$.

(2) $\|T_{zw}(z)\|_\infty<\gamma$, $T_{zw}(z)$ denotes the transfer function from $w$ to $z$

(3) $K(z)$ achieves the robust tracking property for the reference model.

where $w$ is the disturbance input, $u$ is the control input, $z$ is the controlled output, $y$ is the measured output, and $r$ is the reference input.

The $H_\infty$ servo problem is modified as an usual $H_\infty$ control problem with the internal model $\Sigma(z)$ which contains the mode of reference input model. In this paper, we considered the case of step reference input, hence we set $\Sigma(z)$ and the modified generalized plant $\hat{G}(z)$ by

$$\Sigma(z)=\left[\begin{array}{c|c} I_{p2} & I_{p2} \\ \hline I_{p2} & 0 \end{array}\right] \tag{7}$$

$$\hat{G}(z)=\begin{bmatrix} I_{p2} & 0 \\ 0 & I_{p2} \\ 0 & \Sigma(z) \end{bmatrix} G(z)=\left[\begin{array}{cc|c:c} A & 0 & B_1 & B_2 \\ C_2 & I_{p2} & D_{21} & 0 \\ \hline C_1 & 0 & D_{11} & D_{12} \\ \hdashline C_2 & 0 & D_{21} & 0 \\ 0 & I_{p2} & 0 & 0 \end{array}\right] \tag{8}$$

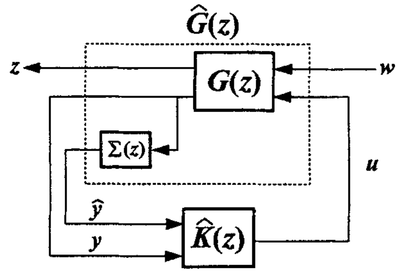


**Fig. 8** $H_\infty$ control problem with the modified generalized plant

The state space realization of $\hat{G}(z)$ in (8) is expressed by

$$\hat{G}(z)=\begin{bmatrix} \hat{G}_{11}(z) & \hat{G}_{12}(z) \\ \hat{G}_{21}(z) & \hat{G}_{22}(z) \end{bmatrix}=\left[\begin{array}{c|cc} \hat{A} & \hat{B}_1 & \hat{B}_2 \\ \hline \hat{C}_1 & \hat{D}_{11} & \hat{D}_{12} \\ \hat{C}_2 & \hat{D}_{21} & 0 \end{array}\right] \tag{9}$$

Consequently, we will solve the following $H_\infty$ control problem in Fig. 8, whose solvability is equivalent to the $H_\infty$ servo problem.

***$H_\infty$* control problem** : For a given generalized plant $G(z)$ in (5) and a reference input $r$, construct the modified generalized plant $\hat{G}(z)$ in (8). Find a controller $\hat{K}(z)$ satisfying the following two specifications.

(1)′ $\hat{K}(z)$ internally stabilizes $\hat{G}(z)$.

(2)′ $\|T'_{zw}(z)\|_\infty<\gamma$, $T'_{zw}(z)$ denotes the transfer function from $w$ to $z$.

The modified generalized plant in (8) does not satisfy the assumptions of the standard $H_\infty$ control problem, such as, $\hat{G}_{12}(z)$ has an imaginary axis zero and $\hat{D}_{21}$ is not of full row rank. Hence, the LMI-based solution to the $H_\infty$ control problem (Gahinet, et al., 1994; Gahinet, 1996) is applied to design the $H_\infty$ servo controller in this paper. For a given $\hat{G}(z)$ and the performance $\gamma$, the discrete-time $H_\infty$ control problem is solvable if and only if there exist two symmetric matrices $R$ and $S$ satisfying the following LMIs.

$$\begin{pmatrix} N_R & 0 \\ 0 & I \end{pmatrix}^T \begin{pmatrix} \hat{A}R\hat{A}^T-R & \hat{A}R\hat{C}_1^T & \hat{B}_1 \\ \hat{C}_1R\hat{A}^T & -\gamma I+\hat{C}_1R\hat{C}_1^T & \hat{D}_{11} \\ \hat{B}_1^T & \hat{D}_{11}^T & -\gamma I \end{pmatrix} \begin{pmatrix} N_R & 0 \\ 0 & I \end{pmatrix}<0 \tag{10}$$

$$\begin{pmatrix} N_S & 0 \\ 0 & I \end{pmatrix}^T \begin{pmatrix} \hat{A}^T S \hat{A} - S & \hat{A}^T S \hat{B}_1 & \hat{C}_1^T \\ \hat{B}_1^T S \hat{A} & -\gamma I + \hat{B}_1^T S \hat{B}_1 & \hat{D}_{11}^T \\ \hat{C}_1 & \hat{D}_{11} & -\gamma I \end{pmatrix} \begin{pmatrix} N_S & 0 \\ 0 & I \end{pmatrix} < 0 \tag{11}$$

$$\begin{pmatrix} R & I \\ I & S \end{pmatrix} > 0 \tag{12}$$

where $N_R$ and $N_S$ denote orthonormal bases of the null spaces of $(\hat{B}_2^T, \hat{D}_{12}^T)$ and $(\hat{C}_2, \hat{D}_{21})$, respectively.

Explicit formulas have been derived for LMI-based $H_\infty$ controllers in discrete time contexts, and they have been successfully implemented in the LMI Control Toolbox for MATLAB (Gahinet, et al., 1995).

### 3.2 $H_\infty$ controller design for the TCM

The $H_\infty$ controller satisfying the following specifications was designed.

1) the robust stability for the variation of friction coefficient between work-roll and strip, and the deformed resistances of strip

2) disturbances attenuation, such as the variation of entry-strip thickness and roll eccentricity

3) robust tracking property for a reference input under the uncertainties.

In this paper, the $H_\infty$ controller of stand 1 was designed, because the strip quality mostly depends on the controller performance of stand 1 in the TCM. The generalized plant $G(z)$ of the $H_\infty$ control is shown in Fig. 9.

In Fig. 9, $G_o$ is the identified nominal model of stand 1, $W_1$ and $W_2$ are the weighting functions, $w$ is the disturbances (the variation of entry-strip thickness and roll eccentricity), $z_1$ and $z_2$ are the controlled output (the delivery-strip thickness, the roll gap and roll speed), $u$ is the control input (the roll gap and roll speed), $y$ is the measured output (the delivery-strip thickness) and $r$ is the reference input (the delivery-strip thickness), respectively.

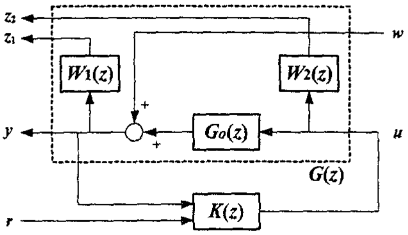


**Fig. 9** Generalized plant for the $H_\infty$ controller of the TCM

### 3.3 Simulation results

Weighting functions for the $H_\infty$ controller of stand 1 were determined by the maximum singular value plot of the modeling error between the nominal model and identified model under uncertainties. The nominal state space models of stand 1 $G_o(z)$ and weighting functions $W_1(z)$, $W_2(z)$ are given by

$$G_o(z) = \left[\begin{array}{c|c} A_o & B_o \\ \hline C_o & D_o \end{array}\right] = \left[\begin{array}{cc|cc} 0.811209 & -0.355172 & -0.168639 & 0.00036 \\ 0.526045 & -0.207644 & -6.619618 & 0.00014 \\ \hline 0.401425 & 0.916641 & -0.010287 & 0.000066 \end{array}\right.$$

$$\left.\begin{array}{cc} -0.013340 & 0.000173 \\ -0.030146 & 0.004366 \\ \hline -0.039681 & 0.000058 \end{array}\right]$$

$$W_1(z) = \left[\begin{array}{c|c} A_{w1} & B_{w1} \\ \hline C_{w1} & D_{w1} \end{array}\right] = \left[\begin{array}{c|c} 0.992519 & 1.0 \\ \hline -0.186561 & 2.493766 \end{array}\right]$$

$$W_2(z) = \left[\begin{array}{c|c} A_{w2} & B_{w2} \\ \hline C_{w2} & D_{w2} \end{array}\right] = \left[\begin{array}{c|c} 0.990050 & 1.0 \\ \hline 0.009901 & 0.004975 \end{array}\right]$$

The designed $H_\infty$ controller of stand 1, which has satisfying disturbances attenuation and robust tracking properties, was assessed in a series of computer simulations with the TCM nonlinear model. Fig. 10(b) shows the disturbance attenuation response of the $H_\infty$ controller of stand 1 under the variation of entry-strip thickness and roll eccentricity shown in Fig. 10(a). A dotted line is the response of stand 1 without any controller and a solid line is the delivery-strip thickness of the $H_\infty$ controller of stand 1. The fluctuation range from 2.12 mm (the set-up value of the

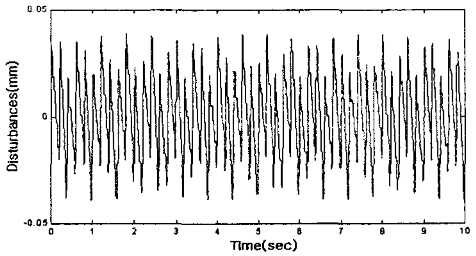


(a) Disturbances : the variation of entry-strip thickness and roll eccentricity

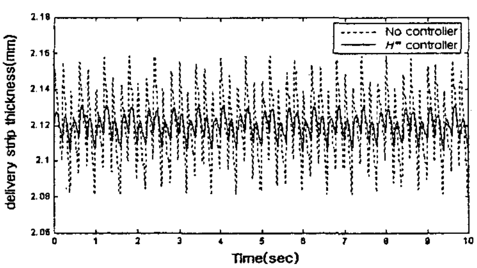


(b) Stand 1 delivery-strip thickness

**Fig. 10** Disturbance attenuation response of the $H_\infty$ controller of stand 1

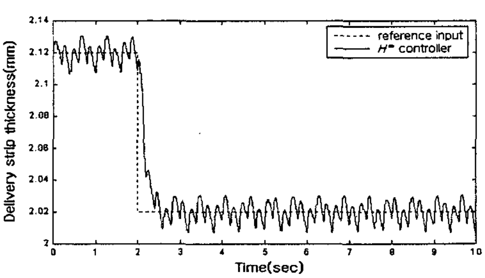


**Fig. 11** Step response of the $H_\infty$ controller under the variation of entry-strip thickness and roll eccentricity

delivery-strip thickness in stand 1) of the $H_\infty$ controller is within $\pm 10$ $\mu$m and the response without controller has the fluctuation range of $\pm 40$ $\mu$m. This comparison shows that the proposed $H_\infty$ controller achieved the disturbance attenuation criterion. In Fig. 11, the step response (decrease from a present thickness of 2.12 mm to a reference thickness of 2.02 mm) of the $H_\infty$ controller in stand 1 is shown. The response reaches the steady state at 2.5 seconds and the fluctuation range of response is within $\pm 10$ $\mu$m.

## 4. Conclusions

In this paper, the control models of the five-stand TCM were constructed using the model identification methods and the $H_\infty$ controller was designed based on the identified model. For model identification, proper input and output variables from the dynamic characteristics analysis of the TCM were selected, and then the input and output data were generated from the nonlinear simulator of the TCM. With the input and output data, the linear models of each stand were identified using the least squares method and the N4SID method. The identified model was evaluated through the comparison to the Taylor linearized model. Finally, the modeling errors of each stand were analyzed in the frequency domain, the robust $H_\infty$ controller was designed with the identified linear model and assessed by computer simulations with the TCM nonlinear model.

## Acknowledgments

This work was supported in part by the POSCO Chair Professor Research Fund of Pusan National University and ERC/Net Shape & Die Manufacturing, and in part by the Brain Korea 21 Project.

## References

Hoshino, I., Meakawa, Y., Fujimoto, T. and Kimura, H., 1997, "Observer-Based Multivariable Control of the Aluminum Cold Tandem Mill," *Automatica*, Vol. 24, No. 6, pp. 741~754.

Lee, M. H. and Hwang, I C., 1998, "A Study of Development of Mathematical Model for Robust Control System of Cold Tandem Mills," *RIMT*, Pusan National University, Technical Report, 1997x006.

Shin, K. H. and Hong, W. K., 1998, "Real-Time Tension Control in a Multi-Stand Rolling System," *KSME International Journal*, Vol. 12, No. 1, pp. 12~21.

Geddes, E. J. M. and Postlethwaite, I., 1998, "Improvements in Product Quality in Tandem Cold Rolling Using Robust Multivariable Control," *IEEE Transactions on Control Systems Technology*, Vol. 6, No. 2, pp. 257~269.

Lee, W. H. and Lee, S. R., 1999, "Computer Simulation of Dynamic Characteristics of Tandem Cold Rolling Process," *KSME International Journal*, Vol. 13, No. 8, pp. 616~624.

Van Overschee and P., De Moor, B., 1994, "N4SID : Subspace Algorithms for the Identification of Combined Deterministic Stochastic Systems," *Automatica*, Vol. 30, No. 1, pp. 75~93.

Verhaegen, M. and Dewilde, P., 1992, "Subspace Model Identification Part 1. The Output Error State Space Model Identification Class of Algorithm," *International Journal of Control*, Vol. 56, No. 5, pp. 1187~1210.

Ljung, L., 1999, *System Identification : Theory for the user*, Prentice Hall.

Hozumi, J., Hara, S. and Fujioka, H., 1997, "Robust Servo Problem with $H_\infty$ Norm Constraint," *International Journal of Control*, Vol. 66, No. 6, pp. 803~823.

Gahinet, P. and Apkarian, P., 1994, "A Linear Matrix Inequality Approach to $H_\infty$ Control," *International Journal of Robust and Nonlinear Control*, Vol. 4, pp. 421~448.

Gahinet, P., 1996, "Explicit Controller Formulas for LMI-based H∞ Synthesis," *Automatica*, Vol. 32, No. 7 pp. 1007~1014.

Gahinet, P., Nemirovski, A., Laub, A. J. and Chilali, M., 1995, *LMI Control Toolbox*, Math Works.